

Supporting Information

Two one-dimensional compounds based on pyramidal {TbCu₄} units and formate ligands: chair-like [(H₂O)₂(ClO₄)₂]²⁻ clusters and slow relaxation of magnetization

Zhong-Yi Li, Jing-Si Yang, Rui-Bin Liu, Jian-Jun Zhang,* Shu-Qin Liu, Jun Ni and Chun-Ying Duan*

Content

Materials and instrumentation	1
Experimental Section	1
Synthesis of compounds	1
X-ray Structure Determinations.....	1
Table S1. Crystal data and structure refinement for 1 and 2	3
Table S2. Selected bond lengths (Å) and angles (°) for 1	4
Table S3. Selected bond lengths (Å) and angles (°) for 2	5
Table S4. Hydrogen bond lengths (Å) and angles (°) for 1	6
Table S5. Hydrogen bond lengths (Å) and angles (°) for 2	7
Scheme S1. Coordination modes of formate and perchlorate in 1 and 2	8
Figure S1. A summary of the structures of the reported inorganic anion-water clusters.....	9
Figure S2. Supplementary figures for the structure of 1 : the coordination polyhedron of the Tb ³⁺ ion	10
Figure S3. Supplementary figures for the structure of 1	11
Description of hydrogen bond networks in 1	12
Figure S4. Supplementary figures for the structure of 2	13
Figure S5. Supplementary figures for the structure of 2	14
Description of hydrogen bond networks in 2	15
Figure S6. Schematic diagrams showing the packing of the chains	16
Figure S7. The IR spectra of 1(a) and 2(b)	17
Figure S8. Powder XRD patterns of 1(a) and 2(b)	18
Figure S9. Field dependence of the magnetization of 1(a) and 2(b) at 1.8K.....	19
Figure S10. <i>M</i> versus <i>H/T</i> plots for 1 at different temperatures below 6 K	20
Figure S11. Temperature dependence of out-of-phase ac susceptibility of 2 under zero dc field.....	20
Figure S12. Temperature dependence of the in-phase (left) and out-of-phase (right) ac susceptibility of 1 under 0.1T dc field	21
Figure S13. Plot of ln($\chi'_M T$) v.s. <i>I/T</i> for 1	21

Materials and instrumentation

All chemicals were obtained from commercial sources and used without further purification. X-ray Powder Diffraction (XRPD) measurements were carried on a Rigaku D/Max-2400 X-ray Diffractometer using Cu K α ($\lambda = 1.5418 \text{ \AA}$) at room temperature. Elemental analyses were determined using a Vario EL III elemental analyzer. FT-IR spectra were recorded in the range of 4000-400 cm⁻¹ on a JASCO FT/IR-430 spectrometer with KBr pellets. Magnetic measurements were performed on a Quantum Design MPMS XL-7. The data was corrected for the sample holder and the diamagnetic contributions.

Experimental Section

Synthesis of [TbCu₄(HCOO)₅(μ₃-OH)₄(H₂O)₈](ClO₄)₂(H₂O)₂ (1):

To an aqueous solution (6 ml) of Tb(ClO₄)₃·6H₂O (1mmol), Cu(ClO₄)₂·6H₂O (741mg, 2mmol) and sodium formate (272mg, 4mmol) were added. Then the pH value of the reaction mixture was carefully adjusted to about 5.5 by slow addition of 0.1 M NaOH solution. After 10 minutes of stirring, the solution was filtrated. Blue crystals were obtained by slow evaporation of the filtrates for a few weeks. Yield: 56% based on Cu. Anal. Calc. for C₅H₂₉Cl₂Cu₄TbO₃₂: C, 5.53; H, 2.69%. Found: C, 5.44; H, 2.67%. IR (KBr) (cm⁻¹): 3417 s, 2882 w, 1567 s, 1394 m, 1352 s, 1114 s, 1086 s, 770w, 627 m, 465w.

Synthesis of [TbCu₄Na₂(HCOO)₄(μ₃-OH)₄(H₂O)₉(ClO₄)₅] (H₂O)₂ (2):

This compound was prepared by following the same procedure as that for **1** but using less amount of sodium formate (136mg, 2mmol). Yield: 43% based on Cu. Anal. Calc. for C₄H₃₀Cl₅Cu₄Na₂O₄₃Tb: C, 3.43; H, 2.16%. Found: C, 3.54; H, 2.11%. IR (KBr)(cm⁻¹): 3416 s, 2879 w, 2022 w, 1573 s, 1391 m, 1365 m, 1145 s, 1113 s, 1088 s, 941w, 776w, 627 m, 494 w.

X-ray Structure Determinations

Intensity data were measured at 293(2) K on a Bruker SMART APEX II CCD area detector system. Data reduction and unit cell refinement were performed with Smart-CCD software ^[1]. The structures were solved by direct methods using SHELXS-97 and were refined by full-matrix least squares methods using SHELXL-97. ^[2]

For **1**, all non-hydrogen atoms were refined anisotropically. The hydrogen atoms related to carbon atoms were generated geometrically. All hydrogen atoms attached to oxygen atoms were located from the difference Fourier map and refined with restrained O-H and H...H distances. The final anisotropic full-matrix least-squares refinement on F² with 256 variables converged to R₁ = 3.45 % for observed data and wR₂ = 8.62 % for all data.

The maximum residual peak and hole on the final difference electron density map were found to be $1.110 \text{ e}^-/\text{\AA}^3$ (1.07 \AA from O12) and $-1.049 \text{ e}^-/\text{\AA}^3$ (0.90 \AA from Tb1), respectively.

For **2**, all non hydrogen atoms were refined anisotropically except oxygen atoms of one ClO_4^- (O20, O21(O21'), O22, O23). One of the oxygen atoms of this ClO_4^- anion is disordered and the occupancy factors are 0.83 for O21 and 0.17 for O21'. The hydrogen atoms related to carbon atoms were generated geometrically. All hydrogen atoms attached to oxygen atoms were located from the difference Fourier map and refined with restrained O-H and H···H distances. The final anisotropic full-matrix least-squares refinement on F^2 with 312 variables converged to $R_1 = 4.04\%$ for observed data and $wR_2 = 11.12\%$ for all data. The maximum residual peak and hole on the final difference electron density map were found to be $1.161 \text{ e}^-/\text{\AA}^3$ (1.39 \AA from O19) and $-0.982 \text{ e}^-/\text{\AA}^3$ (0.64 \AA from O22), respectively.

CCDC 885435 (**1**) and 885436 (**2**) contains the supplementary crystallographic data for this paper. These data can be obtained free of charge via www.ccdc.cam.ac.uk/conts/retrieving.html (or from the Cambridge Crystallographic Data Centre, 12 Union Road, Cambridge CB2 1EZ, UK; fax: (+44) 1223-336-033; or e-mail: deposit@ccdc.cam.ac.uk).

Reference:

- [1] XSCANS (Version 2.1), Siemens Analytical X-Ray Instruments Inc., Madison, WI, **1994**.
- [2] G. M. Sheldrick, *SHELXL-97, Program for X-ray Crystal Structure Refinement*, University of Göttingen: Göttingen, (Germany), **1997**.

Table S1. Crystal data and structure refinement for **1** and **2**.

	1	2
formula	C ₅ H ₂₉ Cl ₂ Cu ₄ O ₃₂ Tb	C ₄ H ₃₀ Cl ₅ Cu ₄ Na ₂ O ₄₃ Tb
Mr.	1085.26	1402.59
Cryst. system	Monoclinic	Monoclinic
space group	P2(1)/m	C2/c
<i>a</i> /Å	8.4356(19)	13.117(4)
<i>b</i> /Å	18.837(4)	14.410(4)
<i>c</i> /Å	10.116(2)	21.239(6)
$\alpha/^\circ$	90	90
$\beta/^\circ$	113.266(2)	102.672(4)
$\gamma/^\circ$	90	90
<i>V</i> (Å ³) / <i>Z</i>	1476.7(6) / 2	3917(2) / 4
<i>d</i> _{calcd.} , g/cm ³	2.441	2.379
F(000)	1060	2744
θ range (°)	2.16~25.00	1.97~25.00
Reflections collected / unique	7209 / 2673	9569 / 3450
R(int)	0.0443	0.0179
Goodness-of-fit on F ²	1.071	1.095
* <i>R</i> 1, (<i>I</i> > 2σ(<i>I</i>))	0.0345	0.0404
** <i>wR</i> 2(all data)	0.0862	0.1112
Max/mean shift in final cycle	0.001/0.000	0.001/0.000

R*1 = $\sum(|F_o| - |F_c|) / \sum |F_o|$, *wR*2 = { $\sum w [(F^2_o - F^2_c)] / \sum w [(F^2_o)^2] \}^{0.5}$, *w* = [$\sigma^2(F^2_o) + (aP)^2 + bP \right]^{-1}$, where *P* = ($F^2_o + 2 F^2_c$)/3. **1**, *a* = 0.0358, *b* = 4.1455; **2**, *a* = 0.0558, *b* = 41.7289.

Table S2. Selected bond lengths (\AA) and angles ($^\circ$) for **1**.

Tb(1)-O(6)	2.402(5)	Cu(1)-O(9)	2.415(6)
Tb(1)-O(14)	2.411(6)	Cu(2)-O(8)	1.952(4)
Tb(1)-O(8)	2.434(4)	Cu(2)-O(7)	1.965(4)
Tb(1)-O(12)	2.436(6)	Cu(2)-O(1)	1.967(4)
Tb(1)-O(13)	2.440(4)	Cu(2)-O(4)	1.984(4)
Tb(1)-O(7)	2.449(4)	Cu(2)-O(10)	2.381(4)
Tb(1)-Cu(3)	3.5007(10)	Cu(3)-O(8)	1.947(4)
Tb(1)-Cu(2)	3.5094(9)	Cu(3)-O(3)	1.964(4)
Cu(1)-O(7)	1.961(4)	Cu(3)-O(5)#2	2.437(6)
Cu(1)-O(2)	1.962(4)		
O(6)-Tb(1)-O(14)	66.7(2)	O(7)-Tb(1)-O(7)#1	64.83(17)
O(6)-Tb(1)-O(8)#1	130.13(14)	O(7)#1-Cu(1)-O(7)	84.1(2)
O(6)-Tb(1)-O(8)	130.13(13)	O(7)#1-Cu(1)-O(2)	175.87(17)
O(14)-Tb(1)-O(8)	75.75(15)	O(7)-Cu(1)-O(2)	92.69(17)
O(8)#1-Tb(1)-O(8)	64.79(17)	O(2)-Cu(1)-O(2)#1	90.4(3)
O(6)-Tb(1)-O(12)	72.0(2)	O(7)-Cu(1)-O(9)	90.85(17)
O(14)-Tb(1)-O(12)	138.6(2)	O(2)-Cu(1)-O(9)	91.75(19)
O(8)-Tb(1)-O(12)	135.92(12)	O(8)-Cu(2)-O(7)	84.29(15)
O(6)-Tb(1)-O(13)	70.47(10)	O(8)-Cu(2)-O(1)	175.93(16)
O(14)-Tb(1)-O(13)	82.97(13)	O(7)-Cu(2)-O(1)	91.90(16)
O(8)#1-Tb(1)-O(13)	136.58(14)	O(8)-Cu(2)-O(4)	94.22(16)
O(8)-Tb(1)-O(13)	73.53(13)	O(7)-Cu(2)-O(4)	174.79(17)
O(12)-Tb(1)-O(13)	83.46(13)	O(1)-Cu(2)-O(4)	89.46(17)
O(13)-Tb(1)-O(13)#1	140.9(2)	O(8)-Cu(2)-O(10)	90.78(15)
O(6)-Tb(1)-O(7)	131.04(13)	O(7)-Cu(2)-O(10)	90.60(15)
O(14)-Tb(1)-O(7)	138.34(12)	O(1)-Cu(2)-O(10)	90.67(17)
O(8)-Tb(1)-O(7)	65.11(12)	O(4)-Cu(2)-O(10)	94.41(17)
O(12)-Tb(1)-O(7)	72.48(14)	O(8)-Cu(3)-O(8)#1	84.1(2)
O(13)-Tb(1)-O(7)	73.06(14)	O(8)-Cu(3)-O(3)#1	177.55(16)
O(13)#1-Tb(1)-O(7)	135.97(14)	O(8)-Cu(3)-O(3)	93.49(17)
O(8)-Tb(1)-O(7)#1	98.83(12)	O(8)-Cu(3)-O(5)#2	83.63(14)
O(8)#1-Cu(3)-O(3)	177.55(16)	O(3)#1-Cu(3)-O(5)#2	95.80(16)
O(3)#1-Cu(3)-O(3)	88.9(3)		

Symmetry codes: #1 x, -y+3/2, z ; #2 x-1, y, z.

Table S3. Selected bond lengths (\AA) and angles ($^\circ$) for **2**.

Tb(1)-O(10)	2.388(5)	Cu(2)-O(1)	1.966(4)
Tb(1)-O(9)	2.417(5)	Cu(2)-O(3)	1.969(4)
Tb(1)-O(11)	2.444(7)	Cu(2)-O(8)	2.304(5)
Tb(1)-O(6)	2.474(4)	Na(1)-O(16)#2	2.385(7)
Tb(1)-O(5)	2.475(4)	Na(1)-O(2)	2.394(5)
Cu(1)-O(6)#1	1.949(4)	Na(1)-O(4)#1	2.471(5)
Cu(1)-O(5)	1.963(4)	Na(1)-O(17)	2.588(9)
Cu(1)-O(2)	1.969(4)	Na(1)-O(20)	2.591(11)
Cu(1)-O(4)#1	1.974(4)	Na(1)-O(13)	2.609(12)
Cu(1)-O(7)	2.345(5)	Na(1)-O(21)	2.64(2)
Cu(2)-O(5)	1.950(4)	Na(1)-O(16)	2.769(9)
Cu(2)-O(6)	1.961(4)	Na(1)-O(14)	2.868(15)
O(10)-Tb(1)-O(10)#1	140.7(2)	O(6)#1-Cu(1)-O(4)#1	93.17(18)
O(10)-Tb(1)-O(9)	85.6(2)	O(2)-Cu(1)-O(4)#1	88.00(18)
O(10)#1-Tb(1)-O(9)	81.69(19)	O(6)#1-Cu(1)-O(7)	93.39(18)
O(9)-Tb(1)-O(9)#1	141.6(2)	O(5)-Cu(1)-O(7)	90.49(18)
O(10)-Tb(1)-O(11)	70.37(12)	O(2)-Cu(1)-O(7)	93.52(19)
O(9)-Tb(1)-O(11)	70.82(12)	O(4)#1-Cu(1)-O(7)	94.1(2)
O(10)-Tb(1)-O(6)#1	138.58(16)	O(5)-Cu(2)-O(6)	83.60(16)
O(9)-Tb(1)-O(6)#1	74.90(16)	O(5)-Cu(2)-O(1)	92.08(18)
O(10)-Tb(1)-O(6)	72.64(15)	O(6)-Cu(2)-O(1)	174.18(18)
O(9)-Tb(1)-O(6)	134.59(15)	O(5)-Cu(2)-O(3)	172.27(17)
O(9)#1-Tb(1)-O(6)	74.90(16)	O(6)-Cu(2)-O(3)	93.06(17)
O(11)-Tb(1)-O(6)	132.23(9)	O(1)-Cu(2)-O(3)	90.75(19)
O(6)#1-Tb(1)-O(6)	95.54(18)	O(5)-Cu(2)-O(8)	95.5(2)
O(10)-Tb(1)-O(5)	75.61(16)	O(6)-Cu(2)-O(8)	93.35(19)
O(10)#1-Tb(1)-O(5)	133.71(16)	O(1)-Cu(2)-O(8)	90.9(2)
O(9)-Tb(1)-O(5)	72.70(15)	O(3)-Cu(2)-O(8)	91.7(2)
O(9)#1-Tb(1)-O(5)	136.89(17)	Cu(2)-O(5)-Cu(1)	106.63(18)
O(11)-Tb(1)-O(5)	131.20(9)	Cu(2)-O(5)-Tb(1)	106.51(16)
O(6)#1-Tb(1)-O(5)	63.87(13)	Cu(1)-O(5)-Tb(1)	105.82(16)
O(6)-Tb(1)-O(5)	63.58(13)	Cu(1)#1-O(6)-Cu(2)	108.97(18)
O(6)#1-Cu(1)-O(5)	84.00(17)	Cu(1)#1-O(6)-Tb(1)	106.31(17)
O(6)#1-Cu(1)-O(2)	172.89(17)	O(5)-Tb(1)-O(5·#1)	97.60(18)
O(5)-Cu(1)-O(2)	94.28(17)	Cu(2)-O(6)-Tb(1)	106.20(16)

Symmetry codes: #1 -x+2, y, -z+1/2; #2 -x+2, -y+2, -z+1.

Table S4. Hydrogen bond lengths (\AA) and bond angles ($^{\circ}$) for **1**.^a

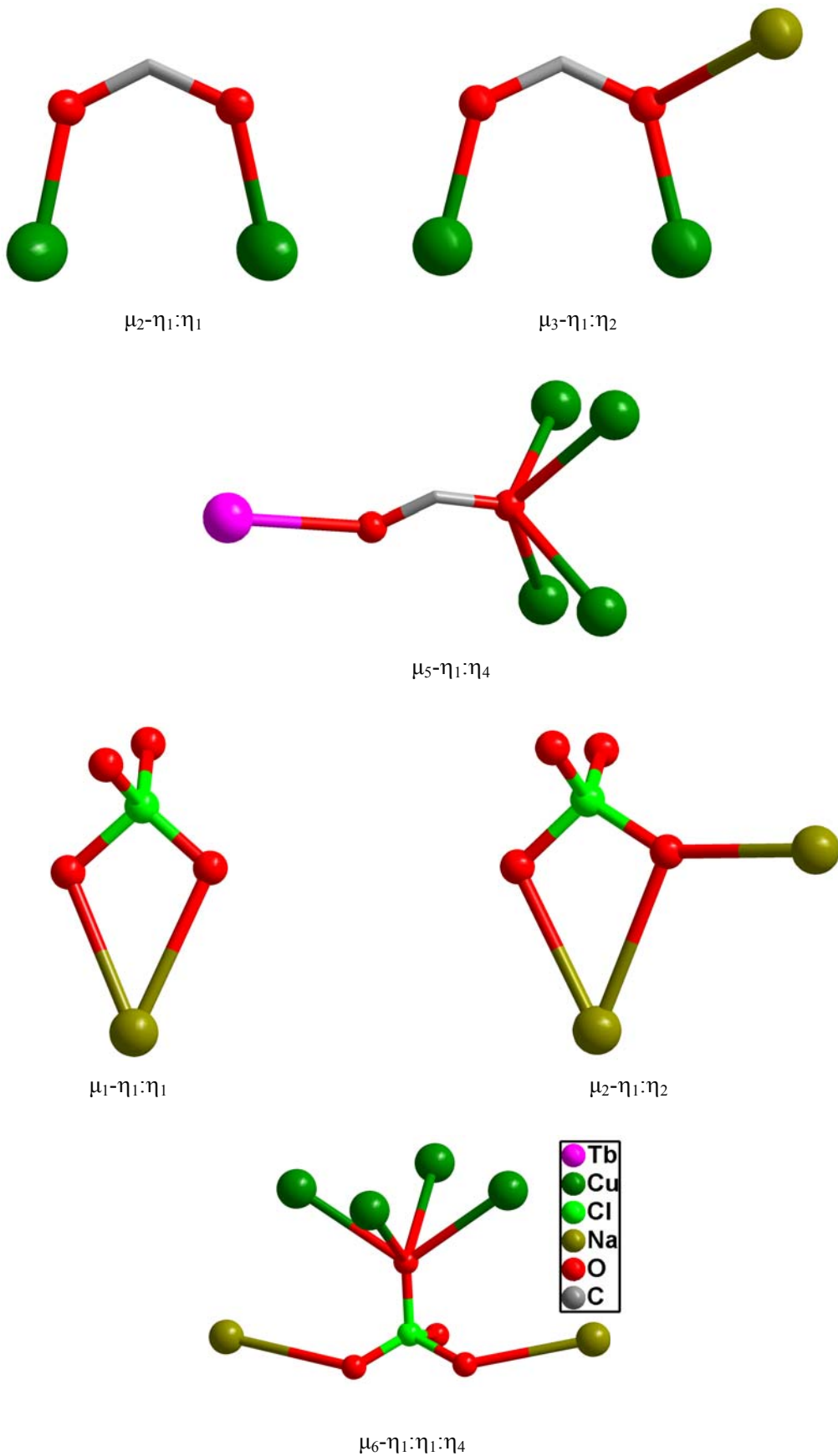
D-H…A	d(D-H)	d(H…A)	d(D…A)	\angle DHA
O7-H7A…O16	0.84(2)	2.05(2)	2.876(7)	170(6)
O8-H8A…O15A	0.84(2)	1.85(2)	2.688(7)	177(6)
O10-H10A…O1B	0.84(2)	2.20(4)	2.862(6)	136(5)
O10-H10B…O4B	0.84(2)	2.13(4)	2.896(6)	152(5)
O11-H11A…O18C	0.84(2)	2.53(3)	3.344(10)	164(8)
O12-H12A…O9	0.85(2)	1.96(3)	2.800(10)	172(8)
O13-H13B…O10	0.86(2)	1.97(2)	2.800(6)	165(6)
O14-H14A…O11	0.85(2)	1.94(3)	2.756(10)	163(8)
O15-H15A…O19	0.85(2)	2.38(7)	3.120(11)	146(10)
O15-H15A…O17	0.85(2)	2.49(6)	3.206(11)	143(8)
O15-H15B…O17D	0.84(2)	2.17(3)	2.980(11)	162(9)
O9-H9A…O3E	0.84(2)	2.18(6)	2.872(7)	139(6)

^a D, donor atom; A, acceptor atom. Symmetry codes: A, -x+2, -y+1, -z+1; B, -x+1, -y+1, -z+1; C, x, y, z+1; D, -x+2, -y+1, -z; E, x, y, z-1.

Table S5. Hydrogen bond lengths (\AA) and bond angles ($^\circ$) for **2**.^a

D-H…A	d(D-H)	d(H…A)	d(D…A)	\angle DHA
O5-H5A…O22A	0.84(2)	2.12(3)	2.938(16)	164(6)
O6-H6A…O18B	0.85(2)	2.03(3)	2.851(9)	163(6)
O7-H7B…O17C	0.85(2)	2.25(5)	2.949(9)	139(7)
O8-H8B…O21A	0.84(2)	2.20(4)	2.98(2)	154(8)
O9-H9A…O24	0.85(2)	2.02(3)	2.825(10)	157(7)
O9-H9B…O7	0.85(2)	2.11(4)	2.896(8)	155(7)
O10-H10A…O3D	0.84(2)	2.12(5)	2.861(6)	147(8)
O10-H10B…O8	0.84(2)	2.09(3)	2.906(8)	163(7)
O11-H11A…O24D	0.81(8)	1.95(8)	2.725(7)	161(9)
O24-H24A…O1E	0.85(2)	2.50(8)	2.916(8)	112(7)
O24-H24B…O19F	0.85(2)	2.22(7)	2.982(12)	150(11)

^a D, donor atom; A, acceptor atom. Symmetry codes: A, x-1/2, y-1/2, z; B, x-1/2, -y+3/2, z-1/2; C, -x+5/2, -y+3/2, -z+1; D, -x+3/2, y-1/2, -z+1/2; E, x+1/2, y-1/2, z; F, -x+2, -y+1, -z+1.



Scheme S1. Coordination modes of formate and perchlorate in **1** and **2**.

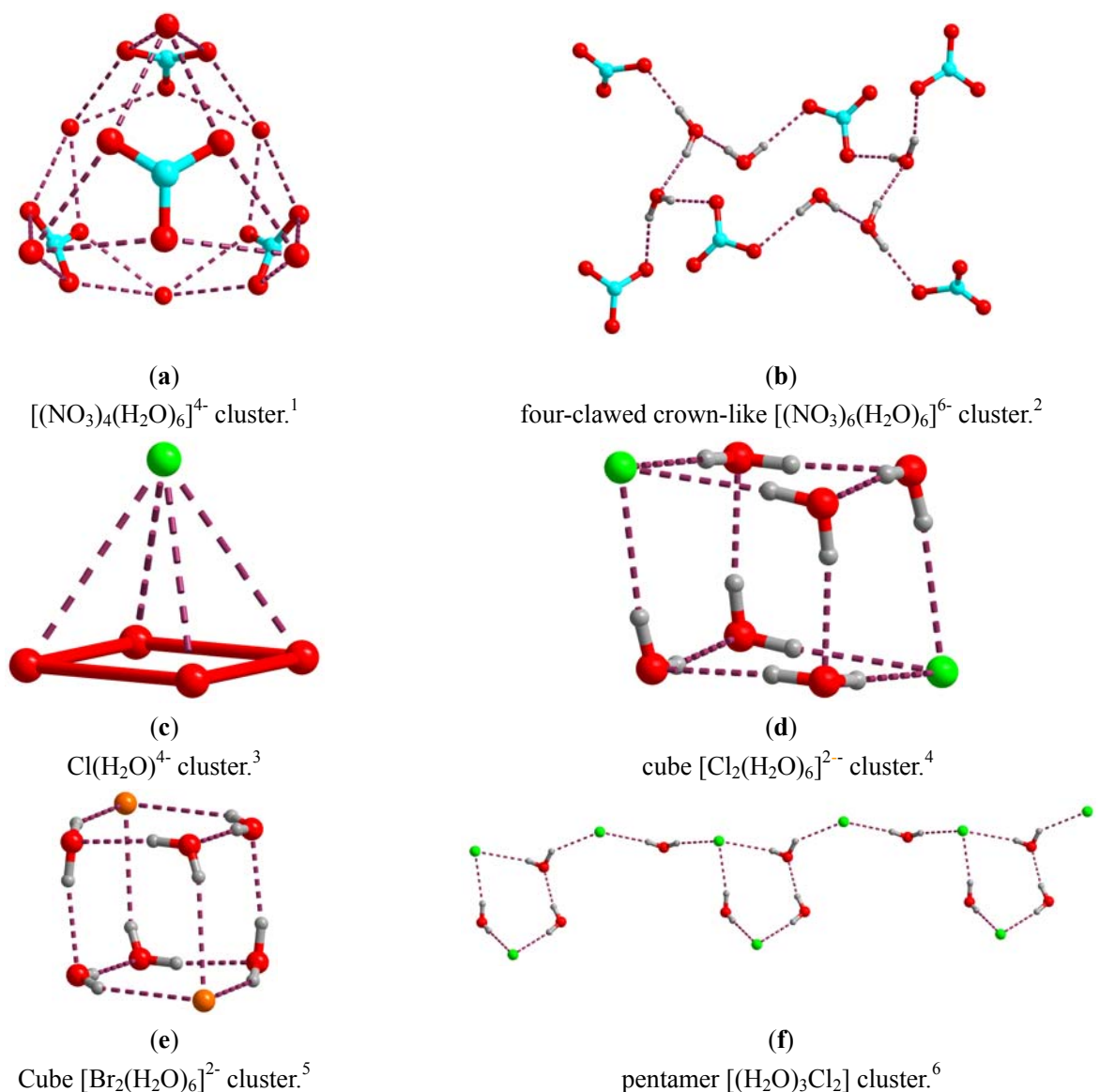


Figure S1. A summary of the structures of the reported inorganic anion-water clusters.

Reference:

- 1 D. Liu, H. X. Li, Z. G. Ren, Y. Chen, Y. Zhang, and J. P. Lang, *Cryst. Growth Des.*, 2009, **9**, 4562.
- 2 L. L. Liu, Z. G. Ren, L. M. Wan, H. Y. Ding and J. P. Lang, *CrystEngComm*, 2011, **13**, 5718.
- 3 R. Custelcean and M. G. Gorbunova, *J. Am. Chem. Soc.*, 2005, **127**, 16362.
- 4 J. R. Butchard, O. J. Curnow, D. J. Garrett and R. G. A. R. MacLagan, *Angew. Chem. Int. Ed.*, 2006, **45**, 7550.
- 5 A. Bakhoda, H. R. Khavasi and N. Safari, *Cryst. Growth Des.*, 2011, **11**, 933.
- 6 M. N. Hoque, A. Basu and G. Das, *Cryst. Growth Des.*, 2012, **12**, 2153.

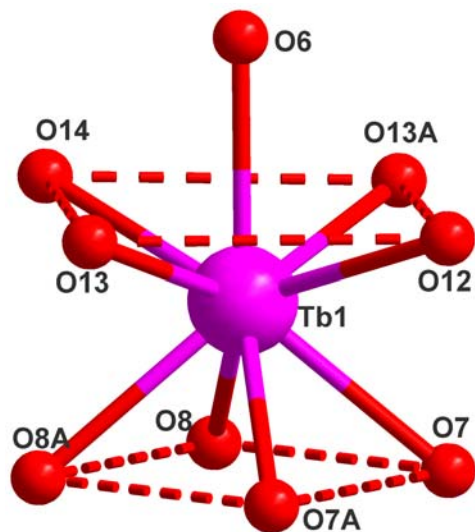


Figure S2. Supplementary figures for the structure of 1: the coordination polyhedron of the Tb^{3+} ion. Symmetry code, A: x, -y+3/2, z.

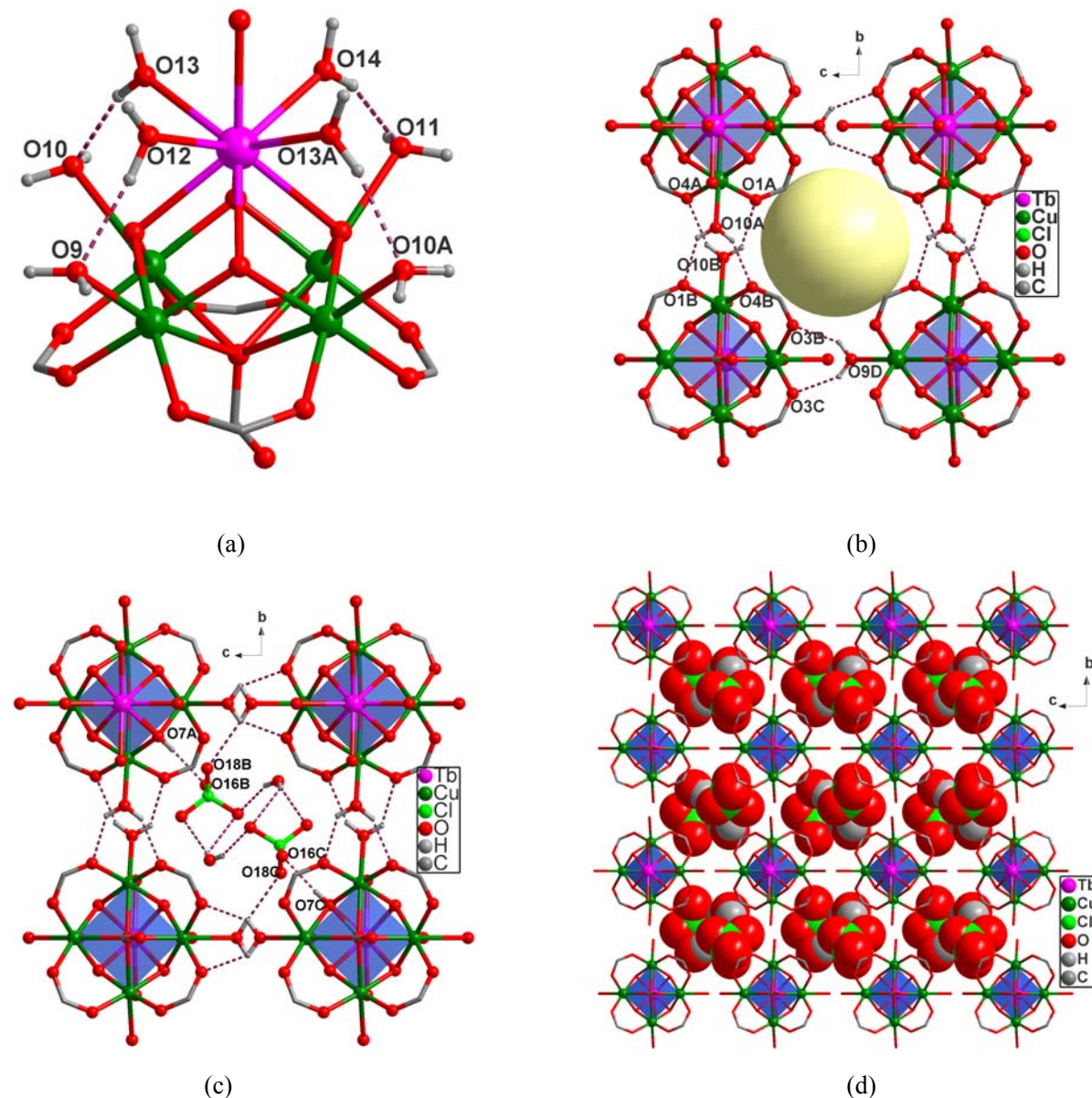


Figure S3. Supplementary figures for the structure of **1**. (a) Hydrogen bond interactions inside the $[\text{TbCu}_4(\text{HCOO})_5(\mu_3-\text{OH})_4(\text{H}_2\text{O})_8]^{2+}$ cluster unit. Symmetry code, A: x, -y+3/2, z; (b) Hydrogen bond networks between the 1D chains and a 3D supramolecular structure is formed. A 1D channel is formed and represented as yellow ball. Symmetry codes: A, -1+x, y, z; B, -x, 1-y, 1-z; C, -x, -0.5+y, 1-z; D, -x, -0.5+y, -z; (c) Hydrogen bond networks between $[(\text{H}_2\text{O})_2(\text{ClO}_4)_2]^{2-}$ clusters and the hydrogen-bonded frameworks. Symmetry codes: A, -1+x, y, z; B, -2+x, y, z; C, -x, 1-y, -z; (d) Packing of the structures viewed along a axis. The $[(\text{H}_2\text{O})_2(\text{ClO}_4)_2]^{2-}$ clusters are shown in space filling mode. Hydrogen bonds are represented as dotted purple line.

Description of hydrogen bond networks in **1**.

A 3D supramolecular structure is formed through complicated hydrogen-bonded interactions. Firstly, inside the $[\text{TbCu}_4(\text{HCOO})_5(\mu_3\text{-OH})_4(\text{H}_2\text{O})_8]^{2+}$ cluster unit, hydrogen bonds between the coordinated water molecules related to Tb^{3+} ion and the coordinated water molecules related to Cu^{2+} ion are formed, as shown in Figure S3a. Secondly, along the *b* direction, adjacent linear chains are associated through interchain hydrogen bonds between the coordinated water molecules (O10) of one chain and formate oxygen atoms of another adjacent chain (O1 and O4), to give infinite 2D sheets. Thirdly, along the *c* direction, hydrogen bonds between the coordinated water molecules (O9) and formate oxygen atoms (O3B and O3C) from adjacent chains further link the neighboring sheets into a 3-D hydrogen-bonded framework with a 1D channel running along the *a* direction (Figure S3b). Fourthly, two symmetric equivalent free water molecules and two perchlorate anions are linked together via $\text{O}-\text{H}\cdots\text{O}$ hydrogen bonds, showing a chair-like arrangement (Fig. 1c). As far as we know, this is the first inorganic anion-water cluster with chair-like configuration, although similar configuration has been observed in several water clusters.^[1] Fifthly, the chair-like $[(\text{H}_2\text{O})_2(\text{ClO}_4)_2]^{2-}$ clusters are further binded to the 3-D hydrogen-bonded framework by hydrogen bonds of O7-H7A \cdots O16 and O11-H11A \cdots O18 (Figure S3c). Details of the hydrogen bond interactions are listed in Table S4. Figure S3d is the 3D packing diagram of **1** viewed along the *a* axis.

References:

- [1] Y. C. Liao, Y. C. Jiang and S. L. Wang, *J. Am. Chem. Soc.*, 2005, **127**, 12794; M. Tadokoro, S. Fukui, T. Kitajima, Y. Nagao, S. Ishimaru, H. Kitagawa, K. Isobee and K. Nakasuji, *Chem. Commun.*, 2006, 1274.

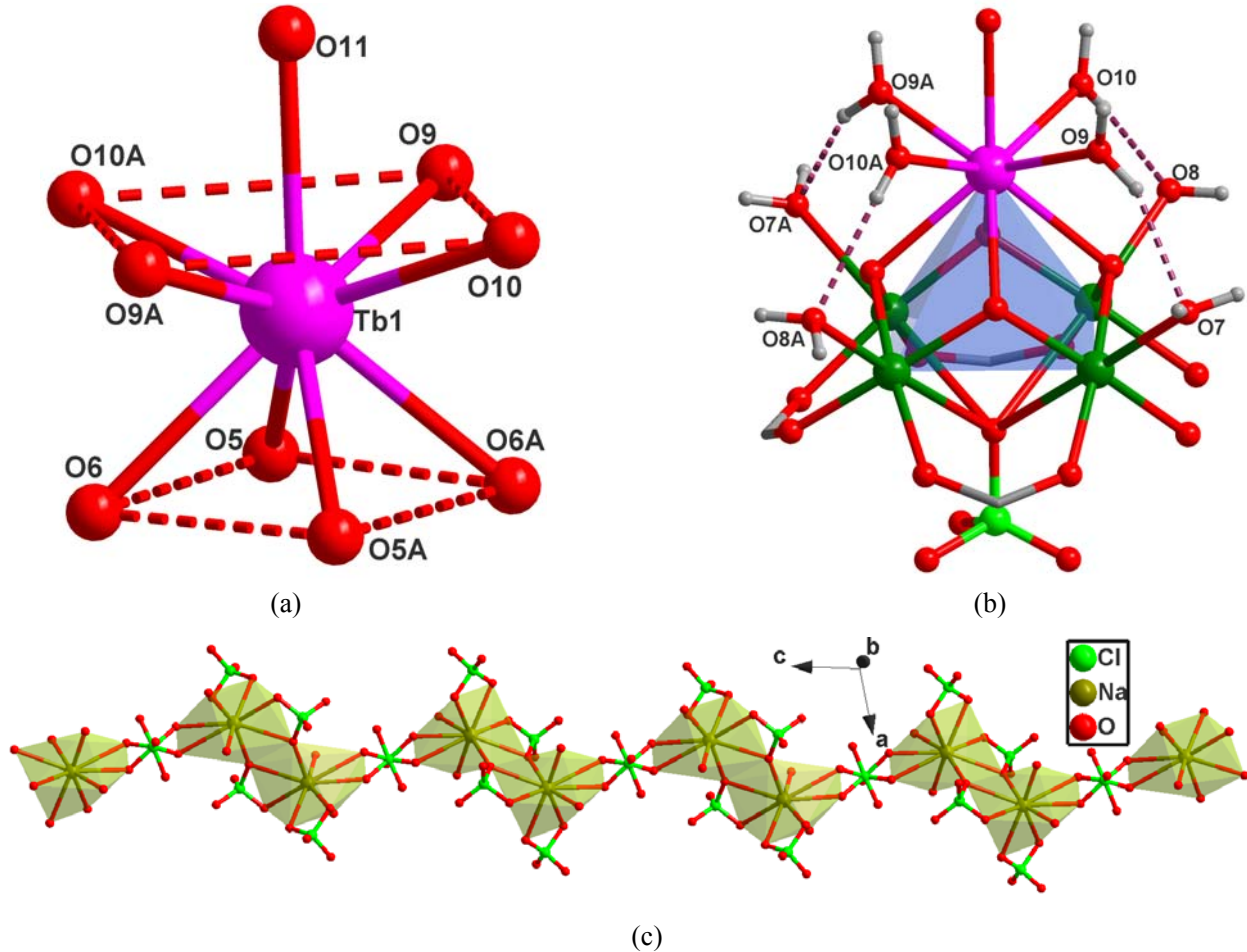


Figure S4. Supplementary figures for the structure of **2**. (a) The coordination polyhedron of the Tb^{3+} ion; (b) Hydrogen bond interactions inside the $[\text{TbCu}_4(\text{HCOO})_4(\mu_3\text{-OH})_4(\text{ClO}_4)(\text{H}_2\text{O})_9]^{2+}$ cluster unit. Symmetry code: 2-x, y, 0.5-z; (c) A 1D chain based on the $[\text{Na}_2(\text{ClO}_4)_4]^{2-}$ building blocks and the μ_6 -coordinated ClO_4^- anions (disordered).

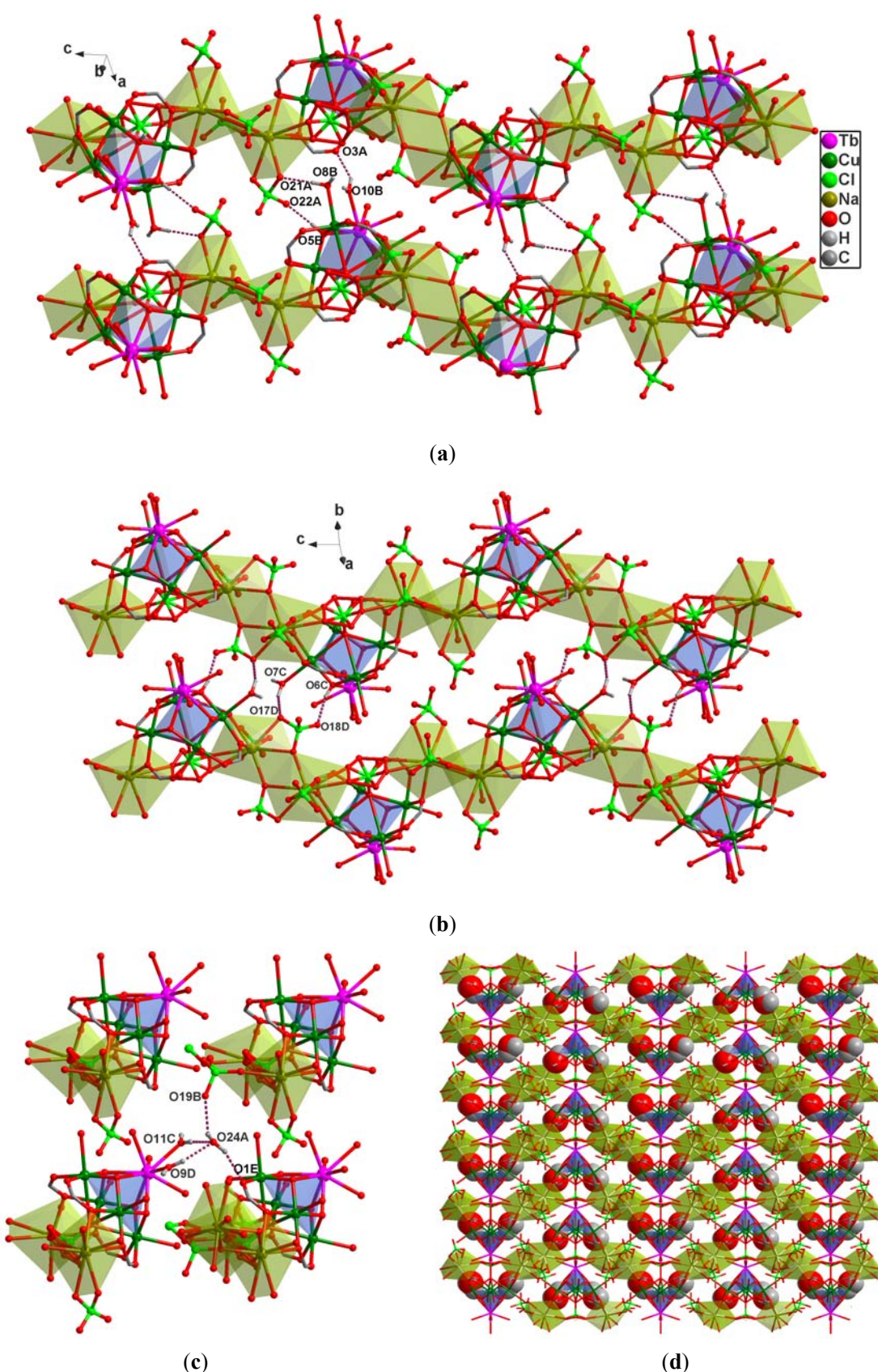


Figure S5. Supplementary figures for the structure of **2**. (a) 2D hydrogen bonded network; (b) 3D hydrogen bonded network. Symmetry codes: A, $1-x$, $-1+y$, $0.5-z$; B, $-0.5+x$, $-0.5+y$, z ; C, $-1+x$, y , $1+z$; D, $1.5-x$, $1.5-y$, $2-z$; (c)

Hydrogen bonds of the free H₂O molecular with the 3D hydrogen bonded framework. Symmetry codes: A, -0.5+x, 0.5-y, 0.5+z; B, 1.5-x, -0.5+y, 1.5-z; C, 1.5-x, 0.5-y, 1-z; D, -0.5+x, 0.5-y, 0.5+z; E, x, 1-y, 0.5-z; (d) Packing of the structures viewed along *a* axis. The free water molecules are shown in space filling mode. Hydrogen bonds are represented as dotted purple line.

Description of hydrogen bond networks in **2**.

Similar to **1**, a 3D supramolecular structure of **2** is formed through complicated hydrogen-bonded interactions. Firstly, as shown in Figure **S4b**, hydrogen bonds between the coordinated water molecules related to Tb³⁺ ion and the coordinated water molecules related to Cu²⁺ ion are formed in the [TbCu₄(HCOO)₄(μ₃-OH)₄(ClO₄)(H₂O)₉]²⁺ cluster unit. Secondly, adjacent zigzag chains are linked through interchain hydrogen bonds of O5-H5A…O22, O8-H8B…O21 and O10-H10A…O3 and give an infinite 2D sheet along the *ac* plane (Figure **S5a**). Thirdly, the neighboring sheets are further connected by the hydrogen bonds of O7-H7B…O17 and O6-H6A…O18 and form a 3D hydrogen-bonded framework (Figure **S5b**). Lastly, the free water molecule (O24) is captured in the 3D hydrogen bonded framework and stabilized by the hydrogen bonds of O9-H9A…O24, O11-H11A…O24, O24-H24A…O1 and O24-H24B…O19 (Figure **S5c**). Figure **S5d** is the 3D packing diagram of **2** viewed along *a* axis. Details of the hydrogen bond interactions are listed in Table **S5**.

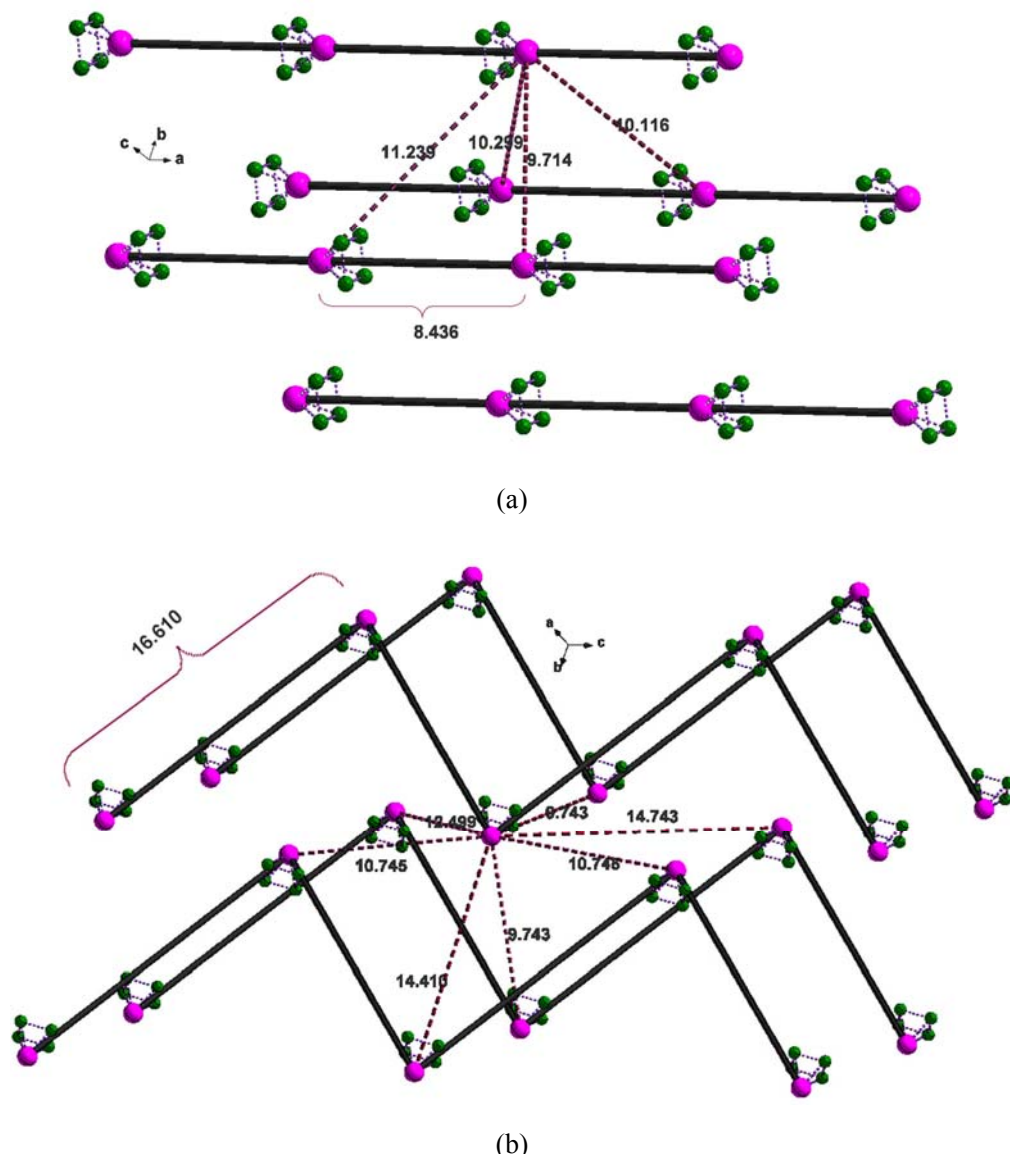


Figure S6. Schematic diagrams showing the packing of the chains. (a) **1**; (b) **2**.

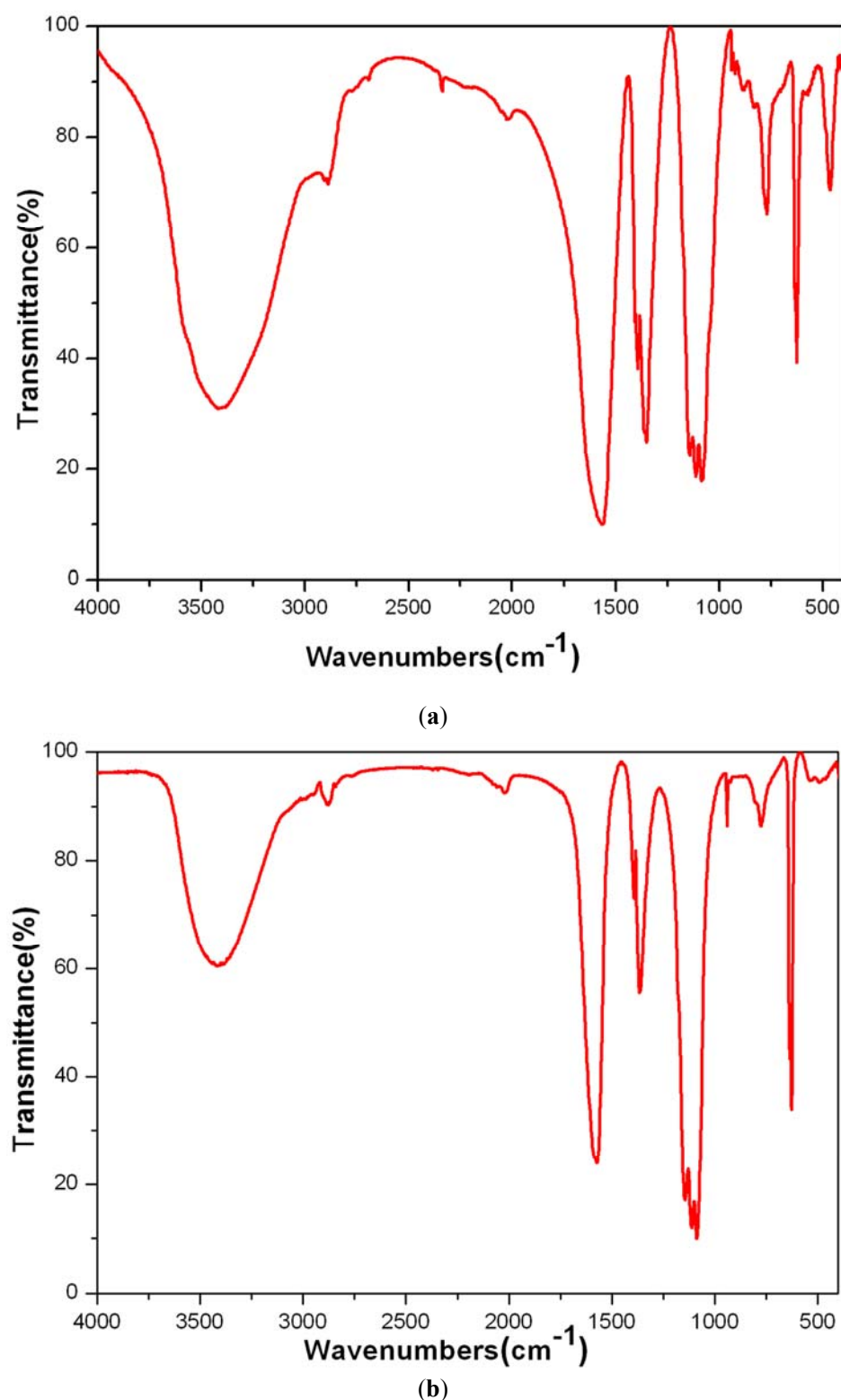


Figure S7. The IR spectra of **1(a)** and **2(b)**.

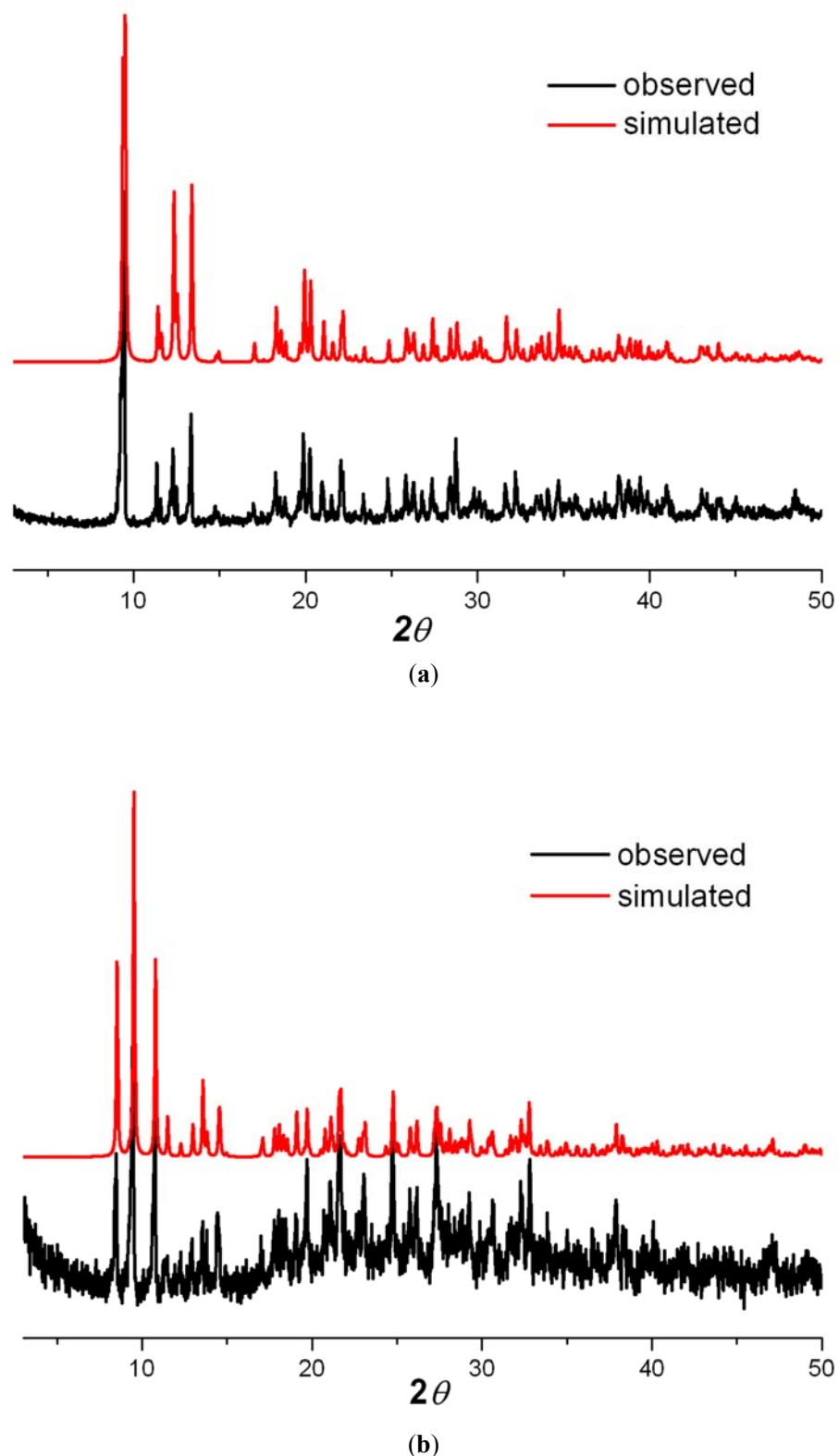
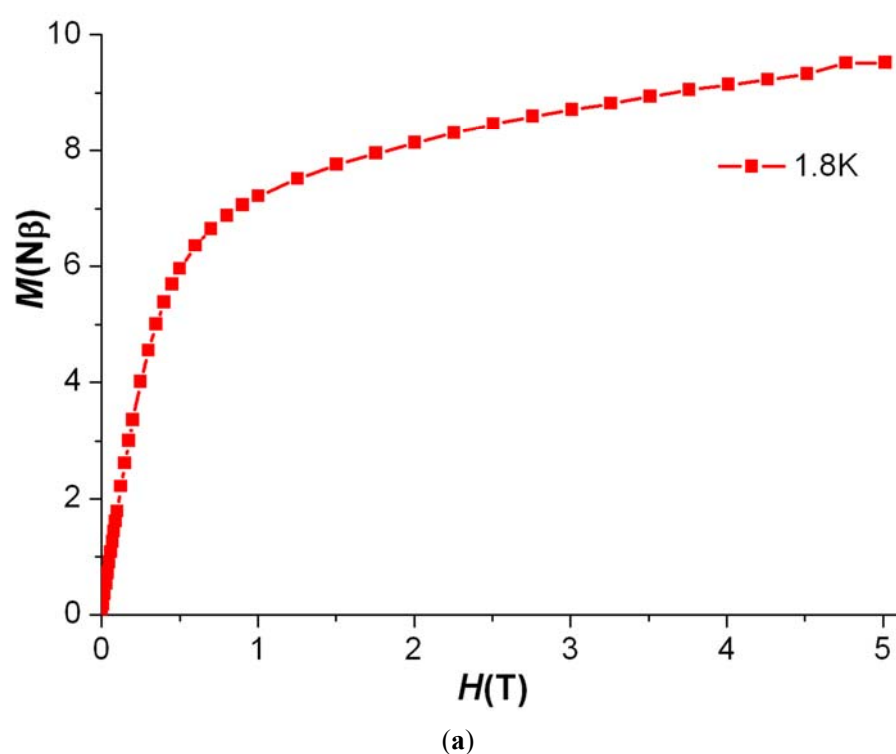
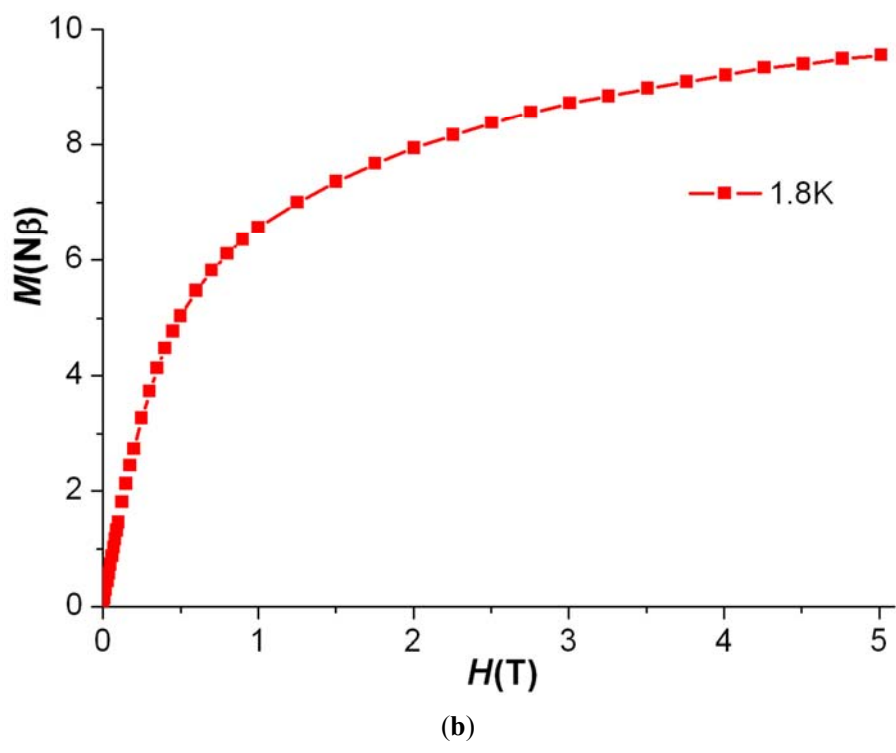


Figure S8. Powder XRD patterns of **1(a)** and **2(b)**.



(a)



(b)

Figure S9. Field dependence of the magnetization of **1(a)** and **2(b)** at 1.8K.

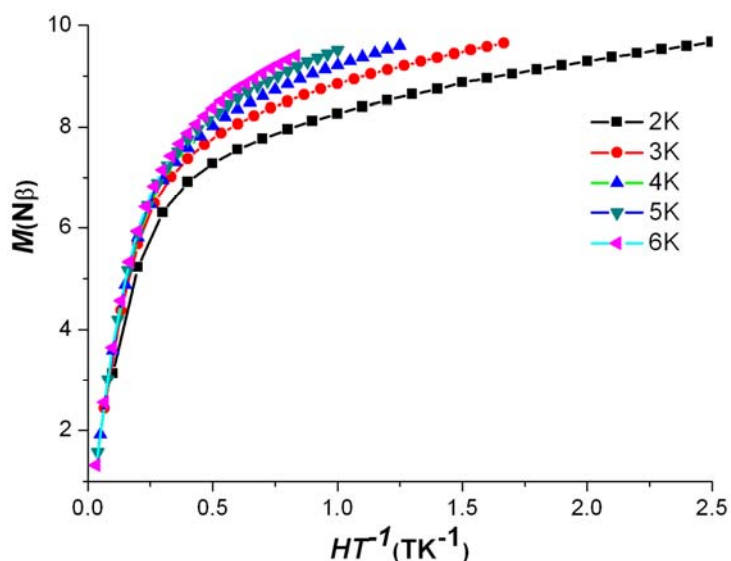


Figure S10. M versus H/T plots for **1** at different temperatures below 6 K.

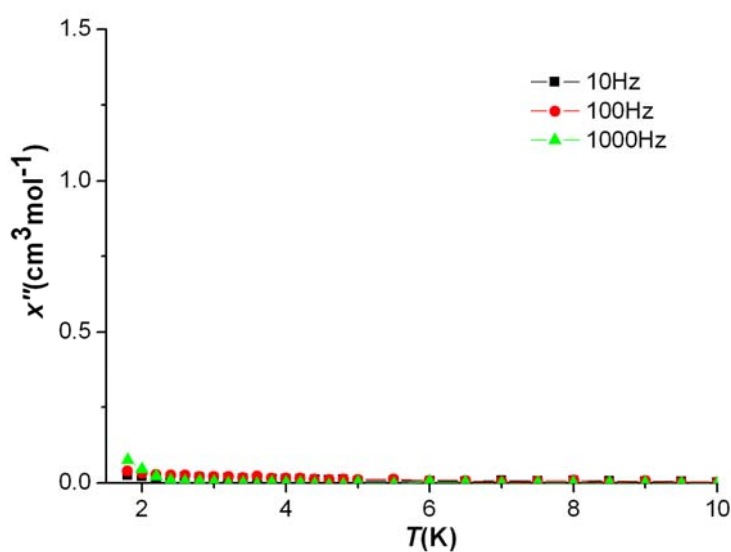


Figure S11. Temperature dependence of out-of-phase ac susceptibility of **2** under zero dc field.

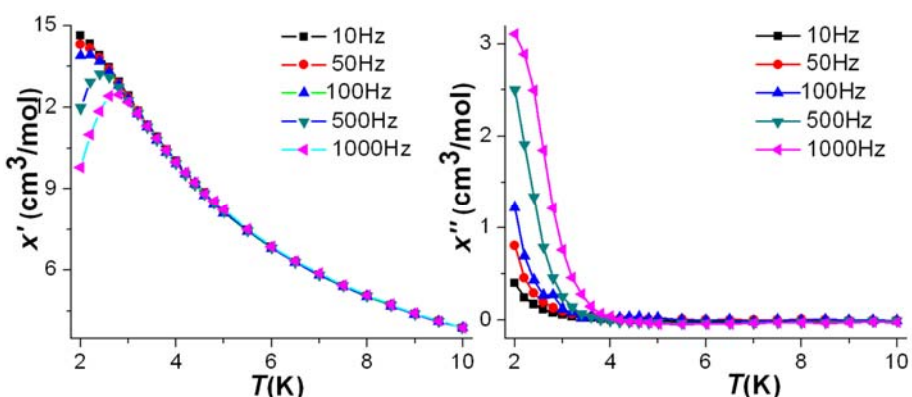


Figure S12. Temperature dependence of the in-phase (left) and out-of-phase (right) ac susceptibility of **1** under 0.1 T dc field.

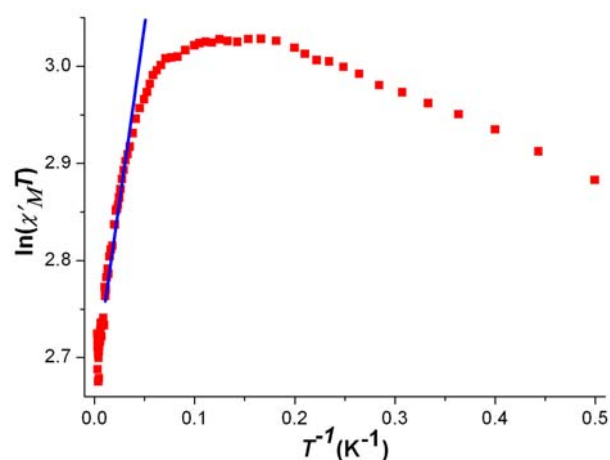


Figure S13. Plot of $\ln(\chi'_M T)$ vs. T^{-1} . The solid line represents the best linear fit in the range 35-70 K. The ac susceptibility data was collected in the temperature range of 2-300 K under a 3.5 Oe ac and zero dc field.